MOEM

Modern Electronic Materials 2024; 10(3): 153–157
DOI 10.3897/j.moem.10.3.135986

Research Article

Atomic and electronic properties of 2D Chevrel phases: A case study of the superatomic two-dimensional semiconductor $Re_6Se_8Cl_2$

Andrey N. Chibisov[1], Daria M. Smotrova[1], Mary A. Chibisova[1], Aleksandr S. Fedorov[2]

1 *Computing Center, Far Eastern Branch of the Russian Academy of Sciences, 65 Kim Yu Chen Str., Khabarovsk 680000, Russian Federation*

2 *Kirensky Institute of Physics, Federal Research Center KSC Siberian Branch Russian Academy of Sciences, 50-38 Akademgorodok, Krasnoyarsk 660036, Russian Federation*

Corresponding author: Andrey N. Chibisov (andreichibisov@yandex.ru)

Received 31 August 2024 ♦ **Accepted** 1 October 2024 ♦ **Published** 9 October 2024

Citation: Chibisov AN, Smotrova DM, Chibisova MA, Fedorov AS (2024) Atomic and electronic properties of 2D Chevrel phases: A case study of the superatomic two-dimensional semiconductor $Re_6Se_8Cl_2$. *Modern Electronic Materials* 10(3): 153–157. https://doi.org/10.3897/j.moem.10.3.135986

Abstract

The design of two-dimensional superatomic materials, which form their atomic structures through covalently bonded clusters with variable chemical compositions, will enable the development of new materials with promised electronic properties that are beneficial for modern nanoelectronics. This paper presents ab initio calculations of the atomic and electronic structures of both bulk and 2D $Re_6Se_8Cl_2$. The calculations were carried out using density functional theory, incorporating noncollinear spin density and the pseudopotential method. The results include data on the atomic structure, band gap value, formation energy of the $Re_6Se_8Cl_2$ 2D layer, and the redistribution of atomic charges within the structures. The differences in effective masses for electrons and holes in the two-dimensional and bulk $Re_6Se_8Cl_2$ materials are demonstrated, along with an explanation of how these differences impact their transport properties. The findings are expected to be of great significance for the design, synthesis, and implementation of new two-dimensional superatomic materials with controlled properties in modern nanoelectronics.

Keywords

superatomic 2D materials, atomic and electronic structure, *ab initio* calculations, band gap, atomic charges, effective masses

1. Introduction

The superatomic compound $Re_6Se_8Cl_2$ is a two-dimensional structural analog of the Chevrel phase materials $M_xMo_6E_8$ (where M = metal, E = S, Se, Te) [1–5]. These materials are referred to as "superatomic crystals" because they are composed of molecular clusters, and some of them are characterized by a layered structure in which $[Re_6Se_8]$ clusters are covalently bonded into layers capped by terminal chlorine atoms [6–8]. In [8], it was demonstrated that strong in-plane intercluster bonding and weak interlayer interactions allow for mechanical exfoliation of $Re_6Se_8Cl_2$ layers. The authors of [8] also showed that bulk $Re_6Se_8Cl_2$ is an indirect bandgap semiconductor with an electronic bandgap of 1.58±0.03 eV, an optical bandgap of 1.48±0.01 eV, and a large exciton binding energy of around 100 meV. Strong coupling of electrons with intercluster optical phonons [9, 10] leads

to the emergence of superconductivity in this material. It was shown that polaron formation protects excitons from scattering by lattice phonons, resulting in quasi-ballistic electron energy transport over several micrometers [10]. Furthermore, an exceptionally long exciton free path of approximately 1 mm was discovered, which opens up the possibility of creating ballistic exciton transistors. In a recent study by Shih et al. [11], it was found that the narrow exciton bandwidth, which can be explained by temperature-dependent renormalization due to optical phonons, plays a crucial role in the stability of acoustic polarons in $Re_6Se_8Cl_2$. Within this mechanism, the polaron binding energy decreases with decreasing temperature.

Transition this material into a two-dimensional state and altering its chemical composition may yield even more intriguing properties, with the potential to design and develop advanced and promising nanoelectronic materials based on it. Therefore, the aim of our research was to theoretically investigate and detail understand the differences in atomic and electronic properties between the bulk and two-dimensional states of $Re_6Se_8Cl_2$.

2. Calculation methods

The calculations of atomic structures and electronic properties were carried out using the VASP package [12–14]. The generalized gradient approximation in the form of GGA–PBE [15] was employed in the PAW pseudopotentials [16, 17]. Spin-orbit coupling and spin polarization were taken into account in the calculations [18]. Van der Waals interactions were included using the Grimme DFT-D3 semi-empirical method [19] to account for interlayer interactions. For testing the properties of the bulk unit cell of $Re_6Se_8Cl_2$, a *k*-point mesh of 9×9×7 was used. For the monolayer, a *k*-point mesh of 9×9×1 was applied using the Monkhorst–Pack scheme [20]. The optimization of the atomic structure was continued until the forces converged to a precision of 10^{-4} eV/nm.

3. Results and discussion

The bulk structure of $Re_6Se_8Cl_2$ is characterized by a triclinic space group P-1, with experimental lattice parameters of a = 0.65784(7) nm, b = 0.66194(8) nm, c = 0.88010(9) nm, and angles α = 76.708(9)°, β = 70.204(9)°, and γ = 86.368(9)° (Fig. 1). The volume of the unit cell is V = 0.35088(6) nm^3 [8]. In our study, a full structural relaxation of the unit cell was performed, maintaining its symmetry while allowing the atomic coordinates to change. As a result, our theoretical calculations yield the following values for the lattice parameters: a = 0.65599 nm, b = 0.66031 nm, and c = 0.87116 nm, with angles α = 76.478°, β = 69.883°, and γ = 86.532°, and a unit cell volume of V = 0.34442 nm^3. Figure 1 shows the bulk unit cell with the specified atomic positions and lattice parameters. The interlayer distance in the $Re_6Se_8Cl_2$

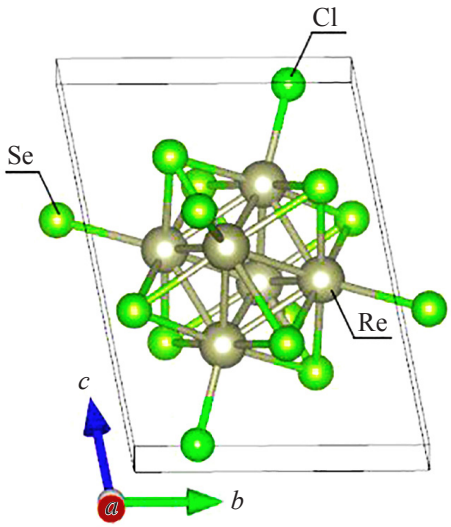

Figure 1. The bulk structure of $Re_6Se_8Cl_2$

unit cell is d = 0.25930 nm. It is evident that our theoretical data agree well with the experimental data, with errors in the lattice constants of only ε_a = 0.28%, ε_b = 0.25%, and ε_c = 1.02%. For the angles, the errors are ε_α = 0.30%, ε_β = 0.46%, and ε_γ = 0.19%, respectively.

To build the most stable 2D layer from the bulk structure of $Re_6Se_8Cl_2$, we used the methodology proposed by Vahdat [21]. This methodology is based on a machine learning approach and allows to determine of the most favorable two-dimensional structure from the three-dimensional bulk material. The resulting 2D layer for $Re_6Se_8Cl_2$ is shown in Fig. 2. Next, the atomic relaxation of the layer was performed, also preserving symmetry and allowing for atomic displacements. For this 2D layer, the equilibrium lattice parameters were determined to be a = 0.65807 nm and b = 0.66075 nm, with angles α = 89.6500°, β = 89.7870°, and γ = 86.0720°. It is observed that during the relaxation of the 2D layer,

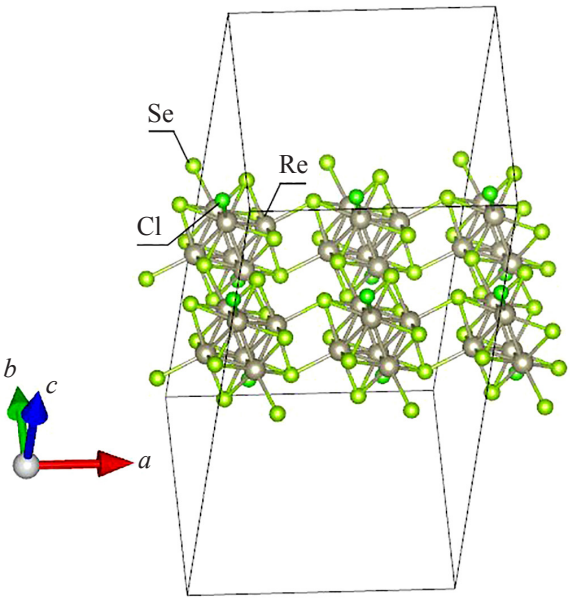

Figure 2. The 2D layer of $Re_6Se_8Cl_2$

to relieve surface stresses, the lattice parameter a changes more significantly compared to parameter b, resulting in an increase in the cross-sectional area in the *XY* plane. To eliminate interactions between $Re_6Se_8Cl_2$ layers during their translation along the *Z*-axis, we set the lattice parameter c to 2.86201 nm. According to our calculations, the formation of a 2D layer from bulk $Re_6Se_8Cl_2$ by mechanical exfoliation requires an energy expenditure of approximately 0.65 eV per formula unit. This energy value was determined using the following expression:

$$E_{form} = E_{2D} - E_{bulk},$$

where E_{2D} is the total energy of the 2D layer of $Re_6Se_8Cl_2$ and E_{bulk} is the total energy of the bulk material [22]. Thus, it is evident that the obtained value for the energy required to form a two-dimensional layer of $Re_6Se_8Cl_2$ is significantly higher than that for the monolayer ReSeCl, which is 0.22 eV/fu [23], and the monolayer $ReSe_2$, which is 0.23 eV/fu [24].

The electronic structure analysis reveals that for the bulk material the bandgap is 1.11 eV and the $Re_6Se_8Cl_2$ is an indirect bandgap semiconductor. The "top" of the valence band is localized at the *k*-point Γ (0, 0, 0), while the "bottom" of the conduction band is located at the *k*-point T (0, 0.444, 0.5) in the Brillouin zone. For the 2D structure of $Re_6Se_8Cl_2$, the bandgap increases to 1.34 eV. Thus, the bandgap of the 2D layer is larger compared to the bulk material. The 2D structure remains an indirect bandgap semiconductor, but the localization of the "top" of the valence band and the "bottom" of the conduction band changes. Specifically, the "top" of the valence band is now located at the *k*-point (0.111, –0.111, 0), while the "bottom" of the conduction band is at the *k*-point (0, –0.444, 0). The obtained bandgap values for both the bulk and 2D $Re_6Se_8Cl_2$ are consistent with other reported data [25]. For an accurate assessment of the bandgap, we employed the local potential approximation (LMBJ-potential) [26, 27], which is optimal for two-dimensional materials.

Table 1. Charges on atoms according to the Bader method in units of electrons (average charge values are provided)

Structure	Re	Se	Cl
2D	–0.596	+0.325	–0.489
bulk	–0.595	+0.318	–0.512

Table 2. Effective masses for electrons (m_e) and holes (m_h) in the bulk and 2D materials

Direction	m_e^*	m_h^*
bulk $Re_6Se_8Cl_2$		
k-path $G \rightarrow X$	$1.571m_0$	$0.701m_0$
k-path $G \rightarrow Y$	$9.545m_0$	$1.105m_0$
2D layer $Re_6Se_8Cl_2$		
k-path $G \rightarrow X$	$1.294m_0$	$1.643m_0$
k-path $G \rightarrow Y$	$5.644m_0$	$2.216m_0$

Next, the analysis of the charge distribution for the $Re_6Se_8Cl_2$ structures was conducted. The charge on the atoms was calculated using the Bader method [28]. It is observed that the charges on the rhenium atoms remain almost unchanged when transitioning from bulk to 2D state. This is likely due to the presence of unpaired electrons on Re atoms, which are shielded by Se atoms through the formation of stable Re–Se bonds [8, 29]. The charge on Se atoms increases by approximately $0.007e$, while the charge on Cl atoms decreases by $0.023e$ (Table 1). This charge transfer influences on the bandgap increase in the two-dimensional structure of $Re_6Se_8Cl_2$. According to Bader's analysis, during forming bulk and 2D materials of $Re_6Se_8Cl_2$ from the chemical elements Re, Se, and Cl, there is a charge transfer from Re atoms to Se and Cl atoms.

Next, to understand the processes of energy and information transfer in these materials, we calculated the effective mass for electrons and holes in the layer planes formed by the $Re_6Se_8Cl_2$ clusters, for both the bulk and 2D materials. We computed the effective masses along the high-symmetry directions $G \rightarrow X$ and $G \rightarrow Y$. For the bulk material, the calculated values are as follows: the effective mass of the electron is $1.571m_0$ and for the hole is $0.701m_0$ along the $G \rightarrow X$ direction, where m_0 is the free electron mass. Along the $G \rightarrow Y$ direction, the effective masses of the electron and hole are $9.545m_0$ and $1.105m_0$, respectively. However, for the 2D material, the effective masses for electrons and holes differ and are as follows: the effective mass of the electron is $1.294m_0$ and for the hole is $1.643m_0$ along the $G \rightarrow X$ direction, while along the $G \rightarrow Y$ direction, the effective masses of the electron and hole are $5.644m_0$ and $2.216m_0$, respectively. Thus, it is evident that the 2D material $Re_6Se_8Cl_2$ exhibits enhanced electron transport properties along the $G \rightarrow X$ direction compared to the bulk material. However, for holes, the transport properties are reduced in both the $G \rightarrow X$ and $G \rightarrow Y$ directions. These results are consistent with those in [10], where the authors first predicted enhanced transport properties for single crystals of $Re_6Se_8Cl_2$. We are the first to show that the 2D materials of $Re_6Se_8Cl_2$ have better electron transport properties compared to the bulk material. Table 2 presents the calculated values for the effective masses of electrons and holes for both the bulk and 2D $Re_6Se_8Cl_2$ materials.

4. Conclusion

In this work, quantum mechanical calculations of the atomic and electronic structure for both bulk and two-dimensional layers of $Re_6Se_8Cl_2$ have been performed. The calculations show that during the relaxation of the 2D layer, to relieve surface stresses, the lattice parameter a changes more significantly (increasing by 0.31%)

compared to parameter *b*, leading to an increase in the surface area of the layer. It is demonstrated the band-gap of the $Re_6Se_8Cl_2$ layer increases comparably to the bulk material, and the 2D structure remains an indirect band-gap semiconductor. Additionally, the charge transfer from Re atoms to Se and Cl atoms occurs during the formation of both the bulk and 2D $Re_6Se_8Cl_2$ materials from the chemical elements Re, Se, and Cl. Analysis of the effective masses for electrons and holes indicates that the 2D material $Re_6Se_8Cl_2$ exhibits enhanced electron transport properties along the $G \rightarrow X$ direction compared to the bulk material. However, for holes, the transport properties are reduced in both the $G \rightarrow X$ and $G \rightarrow Y$ directions.

Acknowledgements

Computations were performed using methods and techniques developed under the State assignment for research work implementation from the Computing Centre Far Eastern Branch of the Russian Academy of Sciences. A.S. Fedorov, who carried out calculations of the carriers effective masses in the materials under study, thanks the state assignment of the L.V. Kirensky Institute of Physics for support. The authors would like to thank them for providing access to the HPC cluster at the Joint Supercom-puter Center of the Russian Academy of Sciences (JSCC RAS).

References

1. Leduc L., Perrin A., Sergent M. Structure du dichlorure et oetaseleniure d'hexarhenium, $Re_6Se_8Cl_2$: Compose bidimensionnel a clusters octaedriques Re_6. *Acta Crystallographica Section C: Structural Chemistry*. 1983; C39: 1503−1506. https://doi.org/10.1107/S010827018300904X
2. Burdett J.K., Lin J.H. Structures of Chevrel phases. *Inorganic Chemistry*. 1982; 21(1): 5−10. https://doi.org/1010.1021/ic00131a002
3. Peña O. Chevrel phases: Past, present and future. *Physica C Superconductivity*. 2015; 514: 95−112. https://doi.org/10.1016/j.physc.2015.02.019
4. Telford E.J., Russell J.C., Swann J.R., Fowler B., Wang X., Lee K., Zangiabadi A., Watanabe K., Taniguchi T., Nuckolls C., Batail P., Zhu X., Malen J.A.,. Dean C.R, Roy X. Doping-induced superconductivity in the van der Waals superatomic crystal $Re_6Se_8Cl_2$. *Nano Letters*. 2020; 20(3): 1718−1724. https://doi.org/10.1021/acs.nanolett.9b04891
5. Kim H., Lee K., Dismukes A.H., Choi B., Roy X., Zhu X., Bonn M. Charge carrier scattering and ultrafast Auger dynamics in two-dimensional superatomic semiconductors. *Applied Physics Letters*. 2020; 116(20): 201109. https://doi.org/10.1063/5.0001839
6. Roy X., Lee C.-H., Crowther A.C., Schenck C.L., Besara T., Lalancette R.A., Siegrist T., Stephens P.W., Brus L.E., Kim P., Steigerwald M.L., Nuckolls C. Nanoscale atoms in solid-state chemistry. *Science*. 2013; 341(6142): 157−160. https://doi.org/10.1126/science.1236259
7. Turkiewicz A., Paley D.W., Besara T., Elbaz G., Pinkard A., Siegrist T., Roy X.J. Assembling hierarchical cluster solids with atomic precision. *Journal of the American Chemical Society*. 2014; 136(45): 15873−15876.
8. Zhong X., Lee K., Choi B., Meggiolaro D., Liu F., Nuckolls C., Pasupathy A., De Angelis F., Batail P., Roy X., Zhu X. Superatomic two-dimensional semiconductor. *Nano Letters*. 2018; 18(2): 1483−1488. https://doi.org/10.1021/acs.nanolett.7b05278
9. Lee K., Maehrlein S.F., Zhong X., Meggiolaro D., Russell J.C., Reed D.A., Choi B., Angelis F.D., Roy X., Zhu X.. Hierarchical coherent phonons in a superatomic semiconductor. *Advanced Materials*. 2019; 31(36): e1903209. https://doi.org/10.1002/adma.201903209
10. Tulyagankhodjaev J.A., Shih P., Yu J., Russell J.C., Chica D.G, Reynoso M.E., Su H., Stenor A.C., Roy X., Berkelbach T.C., Delor M. Room-temperature wavelike exciton transport in a van der Waals superatomic semiconductor. *Science*. 2023; 382: 438–442. https://doi.org/10.48550/arXiv.2306.07808
11. Shih P., Berkelbacha T.C. Theory of acoustic polarons in the two-dimensional SSH model applied to the layered superatomic semiconductor $Re_6Se_8Cl_2$. *The Journal of Chemical Physics*. 2024; 160(20): 204705. https://doi.org/10.1063/5.0205066
12. Kresse G., Hafner J. Ab initio molecular dynamics for liquid metals. *Physical Review B: Condensed Matter and Materials Physics*. 1993; 47(1): 558. https://doi.org/10.1103/physrevb.47.558
13. Kresse G., Furthmüller J. Efficiency of ab-initio total energy calculations for metals and semiconductors using a plane-wave basis set. *Computational Materials Science*. 1996; 6(1): 15–50. https://doi.org/10.1016/0927-0256(96)00008-0
14. Kresse G., Furthmüller J. Efficient iterative schemes for ab initio total-energy calculations using a plane-wave basis set. *Physical Review B: Condensed Matter and Materials Physics*. 1996; 54(16): 11169. https://doi.org/10.1103/PhysRevB.54.11169
15. Perdew J.P., Burke K., Ernzerhof M. Generalized gradient approximation made simple. *Physical Review Letters*. 1996; 77(18): 3865–3868. https://doi.org/10.1103/PhysRevLett.77.3865
16. Blöchl P.E. Projector augmented-wave method. *Physical Review B: Condensed Matter and Materials Physics*. 1994; 50(24): 17953–17979. https://doi.org/10.1103/physrevb.50.17953
17. Kresse G., Joubert D. From ultrasoft pseudopotentials to the projector augmented-wave method. *Physical Review B*. 1999; 59(3): 1758–1775. https://doi.org/10.1103/PhysRevB.59.1758
18. Steiner S., Khmelevskyi S., Marsmann M., Kresse G. Calculation of the magnetic anisotropy with projected-augmented-wave methodology and the case study of disordered $Fe_{1-x}Co_x$ alloys. *Physical Review B: Condensed Matter and Materials Physics*. 2016; 93(22): 224425. https://doi.org/10.1103/PhysRevB.93.224425
19. Grimme S., Ehrlich S., Goerigk L. Effect of the damping function in dispersion corrected density functional theory. *Journal of Computational Chemistry*. 2011; 32(7): 1456. https://doi.org/10.1002/jcc.21759
20. Monkhorst H.J., Pack J.D. Special points for Brillouin-zone integrations. *Physical Review B. Condensed Matter*. 1976; 13(12): 5188. https://doi.org/10.1103/PhysRevB.13.5188

21. Vahdat M.T., Varoon K.A., Pizzi G. Machine-learning accelerated identification of exfoliable two-dimensional materials. *Machine Learning: Science and Technology*.2022; 3(4): 045014. https://doi.org/10.1088/2632-2153/ac9bca
22. Kuklin A.V., Shostak S.A., Kuzubov A.A. Two-dimensional lattices of VN: Emergence of ferromagnetism and half-metallicity on nanoscale. *The Journal of Physical Chemistry Letters*. 2018; 9(6): 1422−1428. https://doi.org/10.1021/acs.jpclett.7b03276
23. 2D Materials Encyclopedia. www.2dmatpedia.org/
24. Hasan N., Sorgenfrei F., Pan N., Phuyal D., Abdel-Hafiez M., Kumar Pal S., Delin A., Thunström P., Sarma D.D., Eriksson O., Karmakar D. Re-dichalcogenides: Resolving conflicts of their structure-property relationship. *Advanced Physics Research*. 2022; 1(1): 2200010. https://doi.org/10.1002/apxr.202200010
25. Le Nagard N., Perrin A., Sergent M., Levy-Clement C. Photoelectrochemical properties of $Re_6Se_8Cl_2$ a lamellar transition metal cluster compound. *Materials Research Bulletin*. 1985; 20(7): 835. https://doi.org/10.1016/0025-5408(85)90063-7
26. Rauch T., Marques M.A.L., Botti S. Local modified Becke-Johnson exchange-correlation potential for interfaces, surfaces, and two-dimensional materials. *Journal of Chemical Theory and Computation.* 2020; 16(4): 2654. https://doi.org/10.1021/acs.jctc.9b01147
27. Rauch T., Marques M.A.L., Botti S. Accurate electronic band gaps of two-dimensional materials from the local modified Becke-Johnson potential. *Physical Review B: Condensed Matter and Materials Physics.* 2020; 101(24): 245163. https://doi.org/10.1103/PhysRevB.101.245163
28. Sanville E., Kenny S.D., Smith R., Henkelman G. Improved grid-based algorithm for bader charge allocation. *Journal of Computational Chemistry*. 2007; 28(5): 899−908. https://doi.org/10.1002/jcc.20575
29. Li Q., Liu F., Russell J.C., Roy X., Zhu X. Strong polaronic effect in a superatomic two-dimensional semiconductor. *The Journal of Chemical Physics.* 2020; 152(17): 171101. https://doi.org/10.1063/5.0006455